

Orbit control on the Pico-Satellite UWE 4 using a NanoFEEP propulsion system and a directive adaptive guidance algorithm

IEPC-2017-389

Presented at the 35th International Electric Propulsion Conference
Georgia Institute of Technology • Atlanta, Georgia • USA
October 8 – 12, 2017

Alexander Kramer¹, Pouyan Azari², Philip Bangert³ and Klaus Schilling⁴
Julius-Maximilians-University, Würzburg, Germany, 97070, Bavaria

The capability of orbit control has not been demonstrated yet in the pico satellite regime. However, this functionality will enable CubeSats for advanced future scientific and industrial applications as a satellite's orbit would not exclusively depend on the insertion by the launcher any more. Additionally, cooperative missions of several small satellites with the capability to keep and change their relative position become feasible. In this study, a variation of the directive adaptive guidance algorithm has been simulated for an acceleration in the order of 10^{-6} m/s², which corresponds to the use-case of a NanoFEEP propulsion system on a pico-satellite. Formulas for the implementation of the algorithm in equinoctial orbital elements are given. In the simulated regime mainly semi-major axis and eccentricity correction result in an appreciable change.

Nomenclature

a	=	semi-major axis
α	=	in-plane thrust angle (pitch)
ADCS	=	attitude determination and control system
β	=	out-of-plane thrust angle (yaw)
COE	=	classical orbital element
DAG	=	directive adaptive guidance
e	=	eccentricity
EO	=	earth observation
i	=	inclination
LPE	=	Lagrange planetary equations
oe	=	orbital element
PPU	=	power processing unit
Ω	=	right ascension of the ascending node
ω	=	argument of perigee
θ	=	true anomaly
RCN	=	radial-circumferential-normal
UWE	=	University Würzburg Experimental Satellite

¹ Department of Computer Science VII: Robotics and Telematics, kramer@informatik.uni-wuerzburg.de.

² Student: Master in Space Science and Technology; Pouyan.azari@uni-wuerzburg.de.

³ Department of Computer Science VII: Robotics and Telematics, bangert@informatik.uni-wuerzburg.de.

⁴ Professor and Chair; Department of Computer Science VII: Robotics and Telematics, schi@informatik.uni-wuerzburg.de.

I. Introduction

SINCE the proposal of the CubeSat standard in 1999 the satellite class has emerged from their initial academic purpose to a whole new industry themselves. Several technologies, like e.g. different communication systems, attitude determination and control systems (ADCS), and Earth observation (EO) nowadays count to the state-of-the-art of pico- and nanosatellite technology^{1,2,*}. With the on-going miniaturization in different fields of terrestrial and space industry the number of applications for these systems continuously increase. With upcoming missions for cooperative small satellites, one major technology which still has to be demonstrated on a pico-satellite scale is propulsion³. Furthermore, those missions often have Earth observation purposes, such that the valuable space at the center of the satellite or the outside panels is needed for the payload and cannot be occupied by the propulsion system.

The University Würzburg Experimental (UWE) Satellite series has put several satellites into orbit since 2005. All UWE satellites follow a roadmap towards formation flying. With the successful in-orbit demonstration of ADCS capabilities on UWE-3^{1,4} an important step towards this goal has been conducted. The following satellite UWE-4 aims at the in-orbit demonstration of a miniaturized Field-emission electric propulsion (NanoFEEP) system⁵ developed by TU Dresden, which is integrated as part of the satellite bus. For the demonstration of orbit control capabilities a directive adaptive guidance (DAG) algorithm⁶ has been implemented and simulated making use of Orekit⁷.

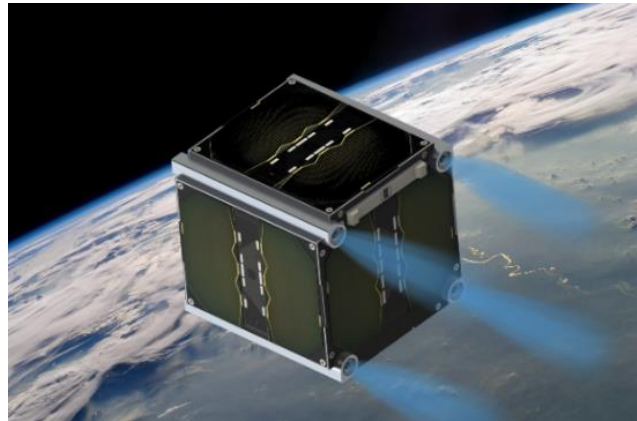


Figure 1. This figure shows a CAD rendered image of UWE-4 with its four thruster heads in the CubeSat bars.

II. UWE-4

The UWE-4 project as a single unit CubeSat project aims on the one hand at the education of students by giving them hands-on experience with satellite technology and on the other hand at the technical objective of demonstrating an electric propulsion system in-orbit. After the successful operation of UWE-3 for almost four years, the design philosophy will also be used in UWE-4. An important lessons learned from previous missions was to implement a system with a high degree of modularity in its architecture in order to account for the participation of students in the form of thesis or project works. The UNISEC standard bus⁸ offers this modularity and additionally a high degree of flexibility in the positioning of the single subsystems within the CubeSat structure. It also already implements redundancy in the communication and power supply lines. This redundancy concept is extended by a redundant electrical power system, on-board data handling system and radio communication subsystem.

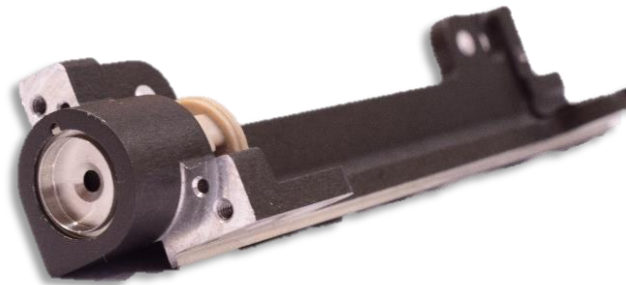


Figure 2. This figure shows an integrated NanoFEEP thruster in a CubeSat bar.

In order to account for the integration of the propulsion system as part of the satellite bus, one thruster head will be placed at the end of each CubeSat bar as can be seen in Fig. 2. The power processing unit (PPU) for the thrusters is developed by TU Dresden as a standard subsystem within the UNISEC bus standard and therefore can be integrated easily. The thruster heads will be connected to the PPU using high voltage cables. This strategy enables to use the propulsion system for 2D attitude control around body x- and y-axis and for orbit control purposes. Additionally the valuable space within the satellite and the outside panels stays unoccupied and can be used for payload in future missions.

* Also refer to NASA's "State of the Art of Small Satellite Technology": <https://sst-soa.arc.nasa.gov>

III. Directive Adaptive Guidance algorithm

The DAG algorithm has been presented first in 2011 by Ruggiero, Pergola, Marcuccio and Adrenucci⁶ and is based on the determination of the thrusting angles at each moment of the orbit in order to create the highest possible rate of change in the desired classical orbital element (COE). The thrusting angles are given in the radial-circumferential-normal (RCN) body frame, where α is the in-plane angle (pitch) and β is the out-of-plane angle (yaw), such that the thrusting vector can be written as in Eq. (1).

$$\vec{f}_{t,oe} = \begin{bmatrix} f_r \\ f_c \\ f_n \end{bmatrix} = |\vec{f}| \begin{bmatrix} \cos(\beta) \sin(\alpha) \\ \cos(\beta) \cos(\alpha) \\ \sin(\beta) \end{bmatrix} \quad (1)$$

In particular, the analytical expressions for the variations of the COEs are derived from the Gauss form of the Lagrange planetary equations (LPE). In order to change several orbital elements simultaneously, a possibility for the combination of the thrusting angles is described. For this purpose an adaptive ratio is introduced as described in Eq. (2).

$$r_{oe} = (oe_t - oe)/(oe_t - oe_0) \quad (2)$$

In Eq. (2) oe , oe_t , and oe_0 are the instantaneous osculating, target and initial value of the specific orbital element (oe). For the purpose of this simulation the osculating element had to be changed to the mean element, since the target orbit lies in the range of the oscillations of the instantaneous osculating elements.

The combined thrust for the change of several orbital elements is originally calculated using Eq. (3)

$$\vec{T} = \sum_{oe} (1 - \delta(oe_t, oe)) r_{oe} \vec{f}_{t,oe} \quad (3)$$

where $\delta(oe_t, oe)$ describes the Kronecker delta and stops the control of the respective orbital element, when the target is achieved. This has also been altered to an ε -vicinity region of the target orbit.

The magnitude of the change of an oe due to thrust applied to the satellite varies within an orbit. Therefore, the authors describe the introduction of maneuver efficiencies making use of the Gauss form of the LPE. The maneuver efficiency is defined as

$$\eta_{oe} = \frac{doe/dt}{(doe/dt)|_{\theta_{max}}} \quad (4)$$

Using this formula a cut-off value can be defined, such that thrust is only applied for the change of an oe, if a certain maneuver efficiency is met and otherwise the satellite coasts for some arc of the orbit.

Introduction of equinoctial orbital elements

However, the COEs have the intrinsic drawback of singularities in Ω and ω for circular and equatorial satellite orbits. For the purpose of an implementation, which can be used as basis in the long run, it should also cover the special cases of circular orbits, which are targeted in future missions⁹. Therefore the algorithm has been implemented using non-singular equinoctial elements¹⁰, as defined in Eqs. (5).

$$\begin{aligned} a &= a \\ P_1 &= e \sin \bar{\omega} \\ P_2 &= e \cos \bar{\omega} \\ Q_1 &= \tan(i/2) \sin \Omega \\ Q_2 &= \tan(i/2) \cos \Omega \\ L &= \bar{\omega} + \theta \end{aligned} \quad (5)$$

with $\bar{\omega} = \omega + \Omega$

In these equations L describes the true longitude. The only remaining singularity occurs for retrograde equatorial orbits, which are not targeted here. Additionally rendezvous and docking is not in the focus of this study, so only the top five equations of Eqs. (5) are important.

The optimal thrusting angles α and β can be computed in equinoctial elements as described in Table 1.

Table 1. This table shows the optimal thrusting angles described in equinoctial elements.

Orbital Element	Pitch α	Yaw β
a	$\tan^{-1}((P_2 \sin(L) - P_1 \cos(L)) / (1 + P_1 \sin(L) + P_2 \cos(L)))$ (6)	0
P_1	$\tan^{-1}(-((1 + P_1 \sin(L) + P_2 \cos(L)) \cos(L)) / (P_1 + (2 + P_1 \sin(L) + P_2 \cos(L)) \sin(L)))$ (7)	$\tan^{-1}(-B/A)$ †
P_2	$\tan^{-1}(((1 + P_1 \sin(L) + P_2 \cos(L)) \sin(L)) / (P_1 + (2 + P_1 \sin(L) + P_2 \cos(L)) \cos(L)))$ (8)	$\tan^{-1}(D/C)$ ‡
Q_1	0	$\pi/2 \cdot \text{sign}(\sin(L) / (1 + P_1 \sin(L) + P_2 \cos(L)))$
Q_2	0	$\pi/2 \cdot \text{sign}(\cos(L) / (1 + P_1 \sin(L) + P_2 \cos(L)))$

IV. Simulation

For the purpose of the implementation of the DAG algorithm the Orekit simulation framework has been used. This simulation makes use of a 10th degree gravitational attraction model¹¹ and an atmosphere model¹² in order to include the perturbing forces which are at the level of the thrust acceleration.

Due to power restrictions of a single unit CubeSat and the specific impulse behavior of the NanoFEEP propulsion system¹³ a maximum thrust of only approx. 7.9 μN can be produced continuously during the mission. With a total satellite mass of approx. 1.33 kg, this leads to a total acceleration of approx. 6 $\mu m/s^2$, which is almost two orders of magnitude below the test case of the original paper⁶.

The start orbit of the simulation is defined using COE of the UWE-3 satellite approximately 1.5 months after the launch at 1st January 2014 midnight⁸. The target COE are defined using COE¹ of the FirstMOVE satellite from TU Munich¹⁴ from the same time, which was deployed from the same deployer in the same launch vehicle in a low-earth orbit. This scenario simulates the compensation of the relative drift between the satellites. The ε -vicinities as stop criterion for the correction of the COE is defined as shown in Table 2.

Table 2. This table shows ε -vicinities of the COEs as stop criterion for the simulation.

COE	a [m]	e [a.u.]	I [deg]
ε -vicinity	100	0.0001	0.0573

A. Single element correction

At first the alteration of a single COE making use of the DAG algorithm is shown in Fig. 3 – the evolution of the other COEs is not considered at this moment.

It can be seen that the semi-major axis is changed quite fast. Already after approximately 6 hours the desired value is reached consuming only 5.1 mg of propellant. This is the most important COE to be altered for the purpose of relative drift compensation.

The progression of the corrected eccentricity clearly shows an alteration in the desired direction. However, the acceleration of the propulsion system is in the range of the gravitational perturbation. Thus the eccentricity reaches its target value faster than naturally, but it needs almost 30 days to perform this change and consumes 321 mg of propellant.

$$^\dagger A = -(1 + P_1 \sin(L) + P_2 \cos(L)) \cos(L) \sin(\alpha) + [P_1 + (2 + P_1 \sin(L) + P_2 \cos(L)) \sin(L)] \cos(\alpha)$$

$$B = P_2(Q_1 \cos(L) - Q_2 \sin(L))$$

$$^\ddagger C = (1 + P_1 \sin(L) + P_2 \cos(L)) \sin(L) \sin(\alpha) + [P_2 + (2 + P_1 \sin(L) + P_2 \cos(L)) \cos(L)] \cos(\alpha)$$

$$D = P_1(Q_1 \cos(L) - Q_2 \sin(L))$$

$$^\S a = 7021.418 \text{ km}, e = 0.00860, i = 97.8727 \text{ deg}, \Omega = 76.8852 \text{ deg}, \omega = 68.1705 \text{ deg}, \theta = 343.8483 \text{ deg}$$

$$^\P a = 7021.057 \text{ km}, e = 0.00902, i = 98.4456 \text{ deg (altered for the purpose of this simulation)}$$

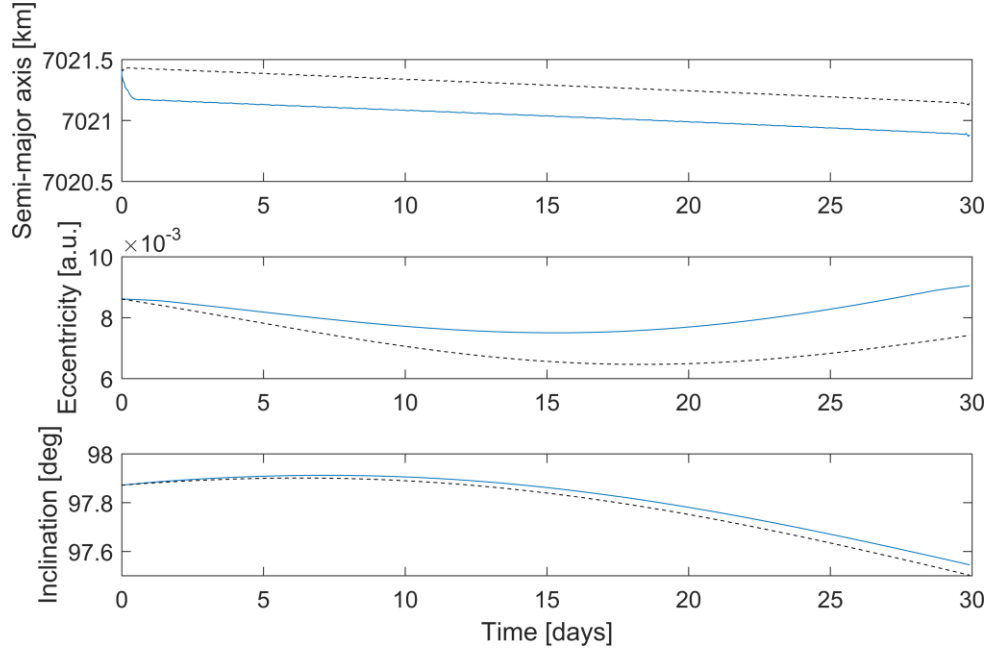


Figure 3. This figure shows the evolution of semi-major axis, eccentricity, and inclination with the DAG algorithm for single element correction (solid blue) in comparison to their natural progression (dashed).

The effect of orbital element correction is even smaller for the inclination. In this case the target value cannot be reached before the satellite runs out of propellant after 93days. For the purpose of illustration only the progression for the first 30days is depicted.

Figure 3 clearly illustrates the necessity to integrate the effect of orbital perturbation into a simulation at this small thrust accelerations in order to achieve realistic results. The gravitational perturbation models can be used to understand the similar magnitude effect of thrust and zonal harmonic terms. The J3 term of the Earth's gravitational model results in a variation of the inclination in the order of

$$|\Delta i_{J3}| \approx 10^{-8} \frac{deg}{s} \quad (9)$$

whereas the propulsion systems effect on the inclination is only in the order of

$$|\Delta i_{thr}| \approx 10^{-9} \frac{deg}{s} \quad (10)$$

The effects of the J2 term of the Earth's gravitational field and the thruster respectively on Ω and ω are shown in Table 3. For this reason it can already be estimated that this COEs will not be effectively altered. Thus the simulation results are omitted here.

Table 3. This table shows magnitude of the effects of J2 and the propulsion system on Ω and ω respectively.

Classical orbital element	Effect of J2 term [rad/s]	Effect of propulsion system [rad/s]
Ω	10^{-6}	10^{-8}
ω	10^{-6}	10^{-9}

B. Combined element correction

The last chapter clarified that only semi-major axis and eccentricity experience an appreciable change due to the maneuvers. For this reason the combined element control of these two COEs has been simulated and is depicted in Fig. 4. The start and target orbits are the same as in the previous chapter. However, the sum of Eq. (3) now comprises of two orbital elements.

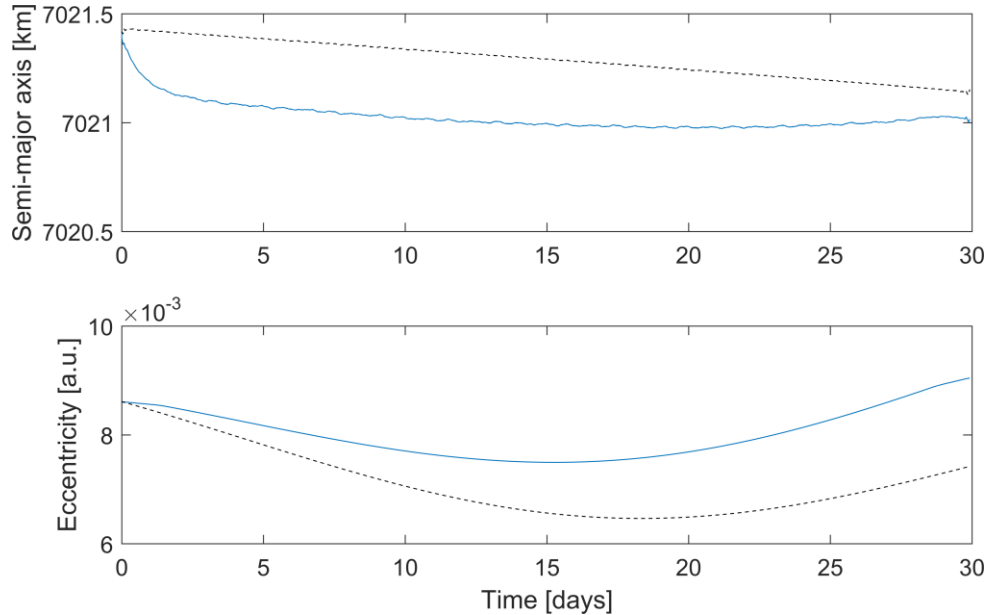


Figure 4. This figure shows the evolution of the semi-major axis and the eccentricity for combined element correction (solid blue) in comparison to their natural progression (dashed).

It can be seen that the semi-major axis converges after approx. 1.3days to its target value and afterwards only corrects the eccentricity, which subsequently reaches its target value after approx. 29days and consumes only 322mg of propellant. This result shows that the combined correction of both elements is more efficient in terms of mass and time than the sum of the correction of the single elements.

V. Conclusion

The simulation results presented in this paper show, that the DAG algorithm in conjunction with an acceleration in the order of $10^{-6} m/s^2$ is capable of changing the semi-major axis, the eccentricity and the inclination of a spacecraft in low-earth orbit. This can be used in order to compensate the relative drift of two satellites which are deployed from the same launch vehicle.

In order to optimize the guidance algorithm for the application of relative drift compensation, the natural progression of the orbit of both spacecraft can be included in the future.

Acknowledgments

The authors appreciated the support for UWE-3 and UWE-4 by the German national space agency DLR (Raumfahrt-Agentur des Deutschen Zentrums für Luft- und Raumfahrt e.V.) by funding from the Federal Ministry of Economics and Technology by approval from German Parliament with reference 50 RU 0901 and 50 RU 1501, respectively, as well as the European Research Council advanced grant NetSat. Furthermore, the authors would like to express their gratitude for the good cooperation with the project partners, notably with Daniel Bock (TU Dresden), Dieter Ziegler (Universität Würzburg), and Stephan Busch (Zentrum für Telematik e.V.).

References

- ¹Busch, S., Bangert, P., and Schilling, K., "Attitude Control Demonstration for Pico-Satellite Formation Flying by UWE-3," in *Small Satellites and Services Symposium - 4S Symposium*, Porto Petro, Mallorca, Spain, 2014.
- ²Trowitzsch, S., Baumann, F., and Brieß, K., "A Picosatellite Demonstrating Three-Axis Attitude Control with Reaction Wheels," in *62. Deutscher Luft- und Raumfahrtkongress*, Stuttgart, Germany, 2013.
- ³Schilling, K., "TIM – A Small Satellite Formation for Earth Observation", *Proceedings of the 9th International Workshop on Satellite Constellations and Formation Flying*, Boulder, Colorado, 2017, IWSCFF 17-67.
- ⁴Bangert, P., Busch, S., and Schilling, K., "Performance Characteristics of the UWE-3 Miniature Attitude Determination and Control system," in *2nd IAA Conference on Dynamics and Control of Space Systems (DYCOSS)*, Rome, Italy, 2014.
- ⁵Bock, D., Kramer, A., Bangert, P., Schilling, K., and Tajmar, M., "NanoFEED on UWE Platform - Formation Flying of CubeSats", presented at the *Joint Conference of 30th ISTS, 34th IEPC, and 6th NSat*, Kobe, Japan, 2015.
- ⁶Ruggiero, A., Pergola, P., Marcuccio, S., and Andrenucci, M., "Low-Thrust Maneuvers for the Efficient Correction of Orbital Elements", presented at the *32nd International Electric Propulsion Conference*, Wiesbaden, Germany, September 2011.
- ⁷Pommier-Maurussane, V., and Maisonobe, L., "Orekit: an Open-source Library for Operational Flight Dynamics Applications", *Proceedings of the International Conference on Astrodynamics Tools and Techniques (ICATT)*, ESA/ESAC, 2010.
- ⁸Busch, S., Bangert, P., Dombrovski, S., and Schilling, K., "UWE-3, in-orbit performance and lessons learned of a modular and flexible satellite bus for future pico-satellite formations, *Acta Astronautica*, Vol. 117. 2015, pp.73-89.
- ⁹Schilling, K., Bangert, P., Busch, S., Dombrovski, S., Freimann, A., Kleinschrodt, A., Kramer, A., Nogueira, T., Ris, D., Scharnagl, J., Tzschichholz, T., „Netsat: A four Pico/Nano-Satellite mission for demonstration of autonomous formation flying, presented at the *66. IAC Congress*, Jerusalem IAC-15-D1.4.2 . 2015.
- ¹⁰Battin, H.R., *An Introduction to the Mathematics and Methods of Astrodynamics*, Revised Edition. American Institute of Aeronautics and Astronautics, 1999. ISBN:1563473429.
- ¹¹Holmes. S.A., Featherstone, W.E., "A unified approach to the Clenshaw summation and the recursive computation of very high degree and order normalised associated Legendre functions", *Journal of Geodesy*, Vol. 76, No. 5, May 2002, pp. 279-299.
- ¹²Montenbruck, O., and Gill, E., *Satellite Orbits*, Springer Verlag, Berlin Heidelberg, 2005, ISBN: 978-3-540-67280-7.
- ¹³Bock, D., Bethge, M., and Tajmar, M., "Highly miniaturized FEED thrusters for CubeSat applications," in *Proceedings of the 4th Spacecraft Propulsion Conference*, Cologne, Germany, 2015.
- ¹⁴Czech, M., Fleischner, A., and Walter, U., „A First-MOVE in Satellite Development at the TU-München“, *Small Satellite Missions for Earth Observation*, Springer, pp. 235-245, 2009.